Plasma Exosomes Contribute to Microvascular Damage in Diabetic Retinopathy by Activating the Classical Complement Pathway

Chao Huang,[1] Kiera P. Fisher,[1] Sandra S. Hammer,[1] Svetlana Navitskaya,[1] Gary J. Blanchard,[2] and Julia V. Busik[1]

Diabetes 2018;67:1639–1649 | https://doi.org/10.2337/db17-1587

Diabetic retinopathy (DR) is a microvascular complication of diabetes and is the leading cause of vision loss in working-age adults. Recent studies have implicated the complement system as a player in the development of vascular damage and progression of DR. However, the role and activation of the complement system in DR are not well understood. Exosomes, small vesicles that are secreted into the extracellular environment, have a cargo of complement proteins in plasma, suggesting that they can participate in causing the vascular damage associated with DR. We demonstrate that IgG-laden exosomes in plasma activate the classical complement pathway and that the quantity of these exosomes is increased in diabetes. Moreover, we show that a lack of IgG in exosomes in diabetic mice results in a reduction in retinal vascular damage. The results of this study demonstrate that complement activation by IgG-laden plasma exosomes could contribute to the development of DR.

Vascular inflammation and activation of the complement system are of significance in many tissues and are especially critical for the brain and retina, where complement activation can disrupt the normal blood-brain and blood-retina barriers (1,2). Because proinflammatory changes contributing to blood-retina barrier breakdown represent an important initiating factor in the pathogenesis of diabetic retinopathy (DR) (3), and because activation of the complement system and impairment of complement regulatory proteins were observed in the eyes of patients with DR and in animal models of DR (1,4,5), this study addressed the role of complement activation in vascular damage in animal and ex vivo models of DR.

The complement system consists of a large group of small, inactive precursors found in the circulation and plays a central role in host defense against infectious pathogens through activation of an inflammatory response. The complement system can be activated through three pathways: the classical, alternative, and lectin pathways. All three of these complement activation pathways lead to generation of C3/C5 convertases and, ultimately, to the formation of the membrane attack complex (MAC). In the classical complement pathway, C1 is the first complement protein that is activated. C1 is a large protein complex comprised of C1q, C1r, and C1s. Downstream proteolytic activation is achieved when C1q binds to a classical activator, such as an Ig complex (6). In DR, elevated complement protein deposition in the retinal vascular lumen has been suggested to be partly due to alternative pathway activation and reduced levels of the complement inhibitor proteins CD55 and CD59 (7,8). Classical pathway complement proteins have not been found in the retinal vascular lumen (8); however, they are significantly elevated in vitreous fluid from patients with DR compared with fluid from age-matched patients without diabetes (9). In addition, the hyperglycemic by-product methylglyoxal has been shown to impair the C1 inhibitor, a circulating regulatory protein belonging to the classical complement pathway (10). Taken together, these studies suggest involvement of the classical complement pathway in the pathogenesis of DR. The mechanism(s) of complement activation and the contribution of complement activation

[1]Department of Physiology, Michigan State University, East Lansing, MI
[2]Department of Chemistry, Michigan State University, East Lansing, MI

Corresponding author: Julia V. Busik, busik@msu.edu.

Received 31 December 2017 and accepted 5 May 2018.

This article contains Supplementary Data online at http://diabetes.diabetesjournals.org/lookup/suppl/doi:10.2337/db17-1587/-/DC1.

to DR pathogenesis remain unknown. It is intriguing that proteomic studies have shown that classical complement proteins such as C1q, C3, and C4 associate with extracellular vesicles such as exosomes in plasma (11–13).

Exosomes are small (40–200 nm in diameter) extracellular vesicles. Exosomes are found in most human biological fluids, including blood (14,15), urine (16), cerebrospinal fluid (17), and ascites (18). Secretion of exosomes initially was proposed as a mechanism to remove unwanted proteins from cells (19). In recent years, however, the role of exosomes has been largely expanded because of their involvement in intercellular communication. Exosomes released from different cells have been shown to carry protein, lipid, and RNA cargo that can affect target cells. For example, in ocular cells, exosomes released from retinal astroglial cells containing antiangiogenic components might serve to protect against neovascularization, whereas exosomes from retinal pigment epithelial cells have not shown this antiangiogenic role (20). In addition to shuttling cytokines and growth factors, exosomes also carry genetic material such as mRNAs, microRNAs, and lipids. It has been suggested that Igs have the capability to associate with exosomes in circulation (21). Igs are potent activators of the classical complement cascade and have been reported to be increased in patients with diabetes compared with patients without diabetes (22). In this study we investigated the role of exosomes in the activation of the classical complement pathway and downstream retinal vascular damage in DR.

RESEARCH DESIGN AND METHODS

Animal Model

All animal procedures complied with the National Institutes of Health *Guide for the Care and Use of Laboratory Animals*, and were approved and monitored by the Institutional Animal Care and Use Committee at Michigan State University. Male C57Bl/6J and Ighm^{tm1cgn}/J (002288) mice, 8 to 12 weeks old, were purchased from The Jackson Laboratory, and diabetes was induced with intraperitoneal doses (55 mg/kg) of streptozotocin (STZ) (Sigma-Aldrich) in 100 mmol/L citric acid (pH 4.5) administered daily for five consecutive days (23). Body weight and blood glucose concentration were monitored twice a week, and blood glucose concentration was maintained around 20 mmol/L. Mice with 7–12 weeks since the onset of diabetes were used in our studies.

Retinal Vascular Permeability

Retinal vascular permeability was analyzed according to a previously published procedure (24).

Western Blot Analysis

Western blot analysis was performed as previously described (25). We used the following antibodies (in a 1:1,000 dilution): anti-CD63, anti-CD9, anti-ALIX, and anti-TSG101 (cat. nos. EXOAB-CD63A-1, EXOAB-CD9A-1, EXOAB-ALIX-1 and EXOAB-TSG101–1, respectively; System Biosciences); anti-C1q (cat. no. A200; Complement Technology, Inc.); anti-C1s (cat. no. A302; Quidel Corp.). As secondary antibodies we used IRDye donkey antirabbit (cat. no. 611-731-127; Rockland Immunochemicals), antigoat (cat. no. 925-32213; LI-COR), and antimouse (cat. no. 610-731-124; Rockland Immunochemicals) antibodies. In experiments with diabetic mice, exosomes isolated from equal volumes (0.1 mL) of control and diabetic plasma were loaded into gel for comparison. Immunoreactive bands were visualized with an Odyssey digital imaging program. We used ImageJ software to quantify the blots.

Exosome Isolation

Blood was collected from the inferior vena cava into EDTA tubes (Microvette 300; SARSTEDT AG & Co.), separated via centrifugation, and either used immediately or aliquoted into 1.5-mL microtubes and stored at −80°C.

The ExoQuick system (System Biosciences) was used to purify plasma exosomes according to the manufacturer's protocol. The ultracentrifugation method to extract exosomes was conducted as previously reported (26). To describe briefly, 0.5 mL plasma was mixed with an equal volume of PBS then centrifuged at 1,000*g* at 4°C for 10 min. The supernatant was saved and spun at 10,000*g* at 4°C for 30 min to remove cellular debris. After the supernatant was filtered through a 0.22-μm filter, exosomes were precipitated by spinning at 100,000*g* at 4°C for 2 h in a Sorvall M120 SE Micro-Ultracentrifuge (S55S-1155 rotor; Thermo Fisher Scientific). The exosome pellet was resuspended in PBS and then either washed by spinning at 100,000*g* or purified with OptiPrep Density Gradient.

Exosome Purification in OptiPrep Density Gradient

Exosomes were purified in OptiPrep Density Gradient as previously described (27), with slight modifications. The exosome mixture (0.08 mL) initially was overlaid on top of a discontinuous gradient, and centrifugation was performed at 100,000*g* at 4°C for 18 h with a Sorvall M120 SE Micro-Ultracentrifuge (S55S-1155 rotor; Thermo Fisher Scientific). Twelve fractions (0.167 mL/fraction) were collected, diluted with 0.833 mL PBS, centrifuged at 100,000*g* at 4°C for 2 h, washed with 1 mL PBS, and then resuspended in 30 μL PBS. Exosomes were identified with Western blotting, on the basis of the exosomal markers CD63, CD9, TSG101, and ALIX, and visualized by electron microscopy. A control OptiPrep gradient containing 0.08 mL buffer (0.25 mol/L sucrose, 10 mmol/L Tris; pH 7.5) was used to determine the density of each fraction (28).

Exosome Quantification

To create a standard curve for use in quantifying plasma exosomes, artificial lipid vesicles were extruded using an Avanti Mini-Extruder (Avanti Polar Lipids, Inc.) with a 0.1-μm polycarbonate membrane. These lipid vesicles were created from 68.3% glycerophospholipid (1,2-dioleoyl-sn-glycero-3-phosphocholine), 22.7% sphingolipid (sphingomyelin), 4.8% glycolipid (1,2-dioleoyl-sn-glycero-3-phosphoglycerol), and 4.3% sterol lipids (cholesterol), as determined previously, in order to mimic the actual composition and size of plasma exosome lipids (29). The actual

concentration of extruded lipid vesicles was calculated using vesicle surface area and composition, and serial dilution was then performed. The extruded lipid vesicles and plasma exosomes then were analyzed with dynamic light scattering (DLS) and static light scattering (SLS) technologies through the use of a Zetasizer Nano NZ (Malvern Instruments Ltd, Malvern, U.K.) to determine both the diameter and the concentration of vesicles, respectively.

Transmission Electron Microscopy

Transmission electron microscopy (TEM) of isolated exosomes was achieved as previously described (26). Immunogold goat antirat antibody (G7035; Sigma) was used for immunogold labeling. Images were taken with a JEM-2200FS Transmission Electron Microscope (ultrahigh resolution; JEOL).

C1q Binding Assay

We performed the C1q binding assay on the basis of previously published procedures (30,31), with modifications. Human or mouse plasma exosomes (isolated from 0.5 mL plasma) were resuspended in 100 μL HEPES buffer (150 mmol/L NaCl, 2 mmol/L $CaCl_2$, 20 mmol/L HEPES; pH 7.0) and incubated with 2 μg C1q (A099; Complement Technology, Inc.) at 37°C for 30 min. The complement activator Heat Aggregated Gamma Globulin (A144; Quidel Corp.) was used as a positive control in the reaction, and C1q alone in the buffer served as the negative control. After incubation, exosomes were isolated via ultracentrifugation, purified in OptiPrep Density Gradient, and analyzed by Western blot.

C1 Activation Assay

The ability of exosomes to induce C1 activation was measured using a previously published in vitro assay (32,33), with modifications. Exosomes was isolated from 0.5 mL human or mouse plasma, resuspended in C1 activation assay buffer (50 nmol/L triethanolamine-HCl, 145 mmol/L NaCl, 1 mmol/L $CaCl_2$; pH 7.4), and incubated with C1 complex (0.25 μmol/L) (A098; Complement Technology, Inc.) in the presence or absence of a C1 inhibitor (INHC1) (A140; Complement Technology, Inc.) at 37°C for 90 min. After incubation, the reaction mixtures were placed on ice for 10 min and purified in OptiPrep Density Gradient; then, we analyzed the activation of C1s using Western blot. The complement activator Heat Aggregated Gamma Globulin (A144; Quidel Corp.) was used as the positive control, and C1 alone in the buffer was the negative control.

Statistical Analysis

The paired Student *t* test was used to analyze data from two groups. For multiple-group comparisons, one-way

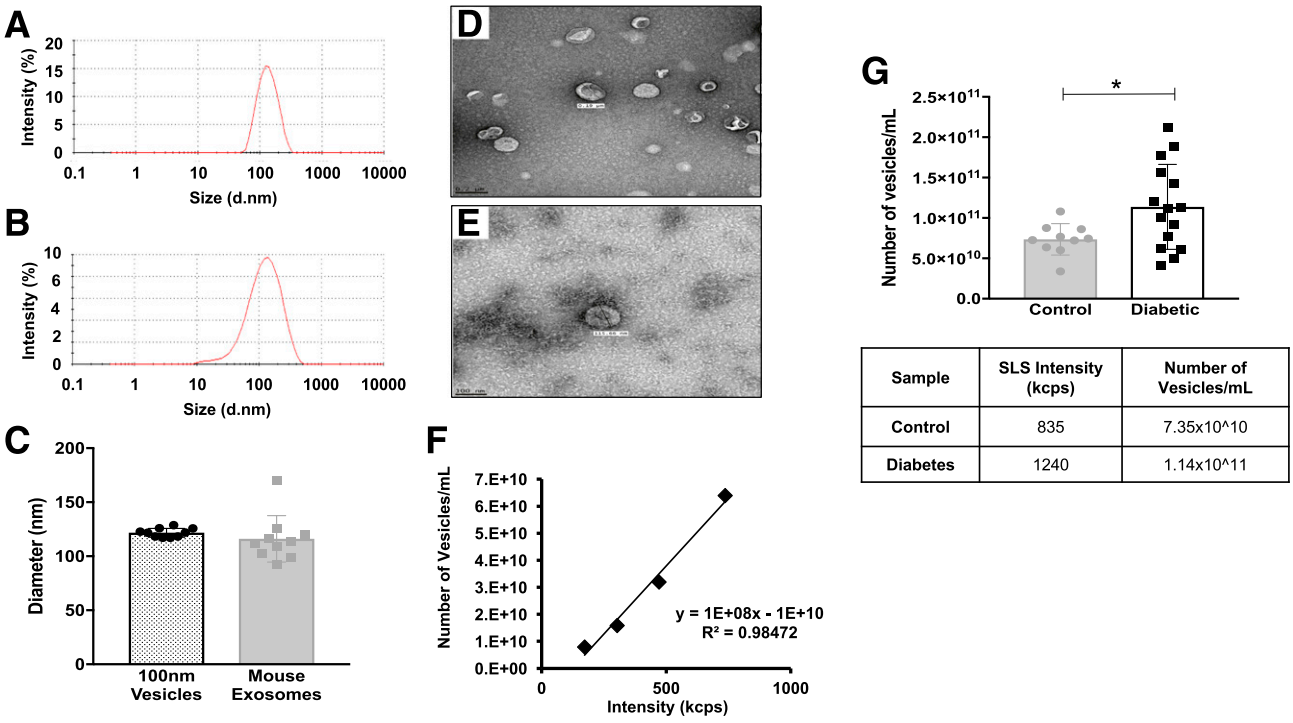

Sample	SLS Intensity (kcps)	Number of Vesicles/mL
Control	835	7.35x10^10
Diabetes	1240	1.14x10^11

Figure 1—Comparison of plasma exosomes, isolated with ExoQuick, and 100-nm extruded microvesicles. *A* and *B*: DLS measurements of 100-nm extruded microvesicles (*A*) and plasma exosomes (*B*). d.nm, diameter, in nanometers. *C*: DLS measurements showed no difference in diameter between 100-nm extruded microvesicles ($n = 9$; dotted bar, black circles) and control mouse exosomes ($n = 10$; gray bar, gray squares). *D* and *E*: Electron microscopy images of 100-nm extruded vesicles (*D*) and plasma exosomes (*E*). Scale bars = 200 nm. *F*: Vesicle concentration (particles per milliliter) plotted against SLS measurement (kilocounts per second [kcps]). *G*: The number of plasma exosomes was increased significantly in diabetic mouse plasma. The number of exosomes isolated from plasma of control mice ($n = 9$; gray bar, gray circles) and STZ-induced diabetic (3 months) mice ($n = 15$; white bar, black squares) was measured through the use of SLS (kilocounts per second) (bottom). All data points are shown as univariate scatter plots with mean and SD. *$P < 0.05$.

ANOVA and post hoc analysis with the Tukey range test were performed using GraphPad Prism 7 software (GraphPad Software, San Diego, CA). All values were expressed as the mean ± SD. P values <0.05 were considered significant.

RESULTS

Quantification of Exosomes in Control and Diabetic Plasma

Quantification of circulating exosomes is challenging because of the lack of stably expressed exosomal markers. In order to achieve the goals of this study, it was important to apply reliable exosome quantification methods; therefore we developed combined DLS and SLS assays using a Zetasizer Nano NZ (Malvern Instruments Ltd.) to quantify and compare the number of exosomes in plasma. Microvesicles of known size, composition, and concentration were extruded using an Avanti Mini-Extruder (Avanti Polar Lipids, Inc.) with 100-nm pore filters; these microvesicles were used to create calibration curves (particles per milliliter). DLS readings of extruded vesicles were compared with DLS readings of isolated mouse plasma exosomes (Fig. 1*A* and *B*). Vesicles extruded through a 100-nm pore filter had a diameter similar to that of mouse plasma exosomes (Fig. 1*C*); this similarity was further confirmed by electron microscopy (Fig. 1*D* and *E*). The absolute concentration of extruded microvesicles was calculated on the basis of lipid composition and vesicle surface area. Serial dilution of 100-nm vesicles, at an initial concentration of 0.64×10^{13} vesicles/mL, was used to generate the calibration curve, which plotted absolute sample concentration (particles per milliliter) against SLS count rate (kilocounts per second) (Fig. 1*F*). The number of circulating exosomes in control and diabetic blood plasma was determined by comparing SLS readings of the plasma exosomes to values on the standard curve created using extruded vesicles of known size and concentration. To prevent sample loss during the ultracentrifugation isolation procedure, exosomes were isolated from an equal volume of mouse plasma (100 μL) by using the ExoQuick precipitation method. We found a significant increase in the concentration of exosomes in plasma from STZ-induced diabetic (3 months) mice compared with that from control mice (Fig. 1*G*). To confirm the SLS result, we analyzed several exosomal markers by Western blot. Under equal volume-loading conditions, exosomal markers CD63, CD9, and TSG101 were more highly expressed in STZ-induced diabetic (3 months) mouse plasma than in plasma from age-matched controls (Fig. 2*A*). We next measured, using DLS, the diameter of exosomes from diabetic mice and those from control mice. We found no difference in the mean diameter between control and diabetic exosomes (Fig. 2*B*). Moreover, CD63 and CD9 expression was not different between control and diabetic exosomes under loading conditions using an equal number of vesicles (Fig. 2*C*). These findings suggest that more circulating exosomes exist in diabetic plasma than in control plasma; furthermore, the size and composition of exosomes are less affected by diabetes.

Igs Are Associated With Exosomes in Plasma

As shown in Fig. 3*A*, we detected an enrichment of exosomal markers and a large amount of IgG in ExoQuick-isolated mouse plasma exosomes (Fig. 3*A*, left lane). Concurrently, we also detected nonexosomal markers such as LDL (apolipoprotein [Apo] E), HDL (ApoA), and endoplasmic reticulum markers (calnexin) in ExoQuick-isolated exosomes. Several reports have shown that ExoQuick and other polymer-based exosome isolation methods coprecipitate other proteins or vesicles such as lipoproteins (34,35), and further separation by centrifugation with OptiPrep Density Gradient is required to obtain pure exosomes (31,32). To confirm that Igs are associated with plasma exosomes, mouse plasma exosomes isolated by ExoQuick were further purified via centrifugation with OptiPrep Density Gradient, and then evaluated with Western blot using exosome markers CD63, CD9, and TSG101. Consistent with previously reported plasma exosomal density ranges (14,26), OptiPrep gradient separation yielded mouse plasma exosomes in fractions 8–10, with a density ranging from 1.16 to 1.39 g/mL (Fig. 3*B*). We detected prominent bands of IgG in the same fractions in which exosomes were present (Fig. 3*B*, bottom). After depleting exosomes from mouse plasma by repeating ultracentrifugation, we found a concomitant reduction of IgG level in exosome-depleted mouse plasma (Fig. 3*C*, right lane). These results suggest that most Igs in circulation are associated with exosomes.

Ultracentrifugation remains the "gold standard" for isolating exosomes, and fewer contaminants are reported with this method than with the ExoQuick method (36). To confirm that IgG associates with exosomes in circulation, ultracentrifugation-isolated rat exosomes were stained with immunogold-labeled IgG and investigated under TEM. Exosomes appeared as disklike shapes with a diameter of ∼150 nm (Fig. 4*A*). TEM showed a strong association of immunogold-labeled IgG with the rat plasma exosomes (Fig. 4*B*). It is interesting to note that an increase in the number of circulating exosomes in diabetic animals was associated with an increase in IgG levels in diabetic mouse samples. This increase in IgG was measured via Western blot analysis under equal volume-loading conditions (Fig. 4*C*), but it was not observed under loading conditions using an equal number of vesicles (Supplementary Fig. 1). These data confirm that it is an elevated number of circulating vesicles, and not a change in exosome morphology, that results in higher IgG levels in diabetic exosome samples when compared with nondiabetic controls.

Circulating Ig Bound to Exosomes Activates the C1 Complex

The C1q binding assay (37) was performed to examine whether the complement cascade can be activated by Ig-associated exosomes. Mouse plasma exosomes were used in this assay, and the results were confirmed through the use of nondiabetic human plasma. Purified human C1q

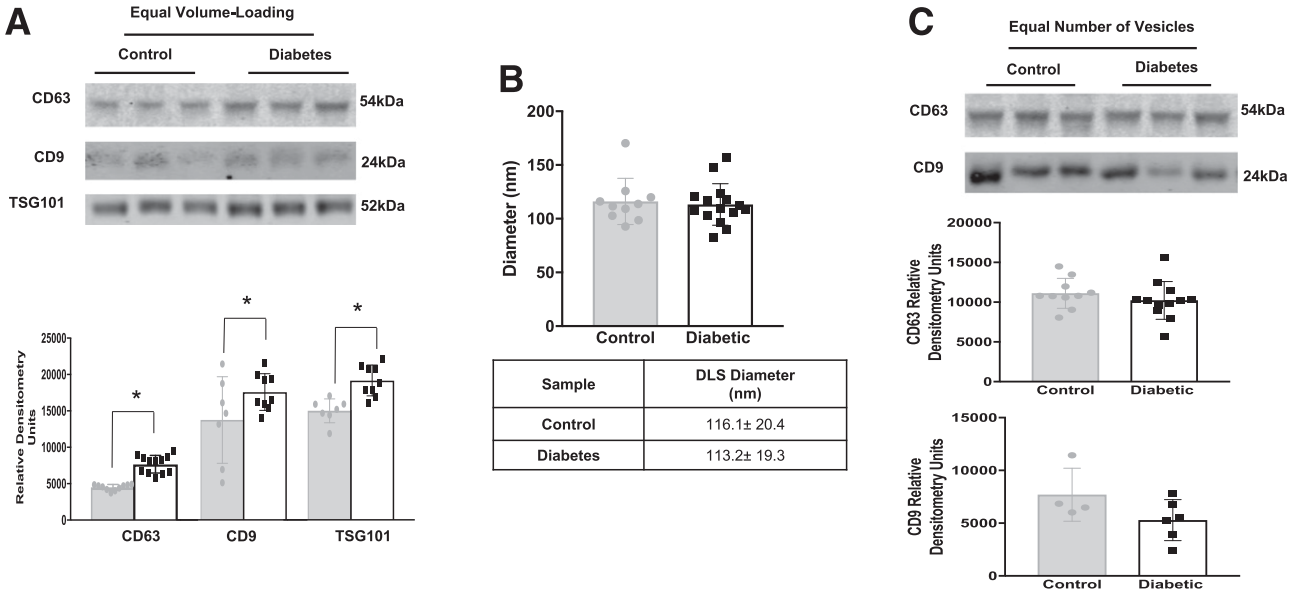

Figure 2—*A*: Western blot of plasma exosomes isolated through the use of ExoQuick from control and STZ-induced diabetic (3 months) mice (top). Under conditions of equal volume, increased amounts of exosomal markers (CD63, CD9, and TSG101) were measured in diabetic mouse plasma (bottom). The markers were quantified on the basis of average band intensity (n = 9, 8, and 7 for the three control measurements (gray bars, gray circles, left to right), and n = 15, 9, and 9 for diabetes measurements (white bars, black squares, left to right). *$P < 0.05$. *B*: DLS (nanometer) readings of mouse plasma exosomes showed no change in exosome diameter between control mice (n = 10; gray bars, gray circles) and diabetic mice (n = 15; white bars, black squares). *C*: Western blot of plasma exosomes isolated with ExoQuick from control and STZ-induced diabetic (3 months) mice. Under loading conditions with an equal number of vesicles, no change in plasma exosomes (CD63 and CD9) was observed between control mice (gray bars, gray circles) and diabetic mice (white bars, black squares). Exosomes were quantified on the basis of average band intensity (n = 10 [middle] and 4 [bottom] for control and n = 12 [middle] and 6 [bottom] for diabetes). All data points are shown as univariate scatter plots with mean and SD.

protein (A099; Complement Technology, Inc.) was incubated with isolated exosomes and purified via centrifugation with the OptiPrep gradient. As shown in Fig. 5*A*, exogenous human C1q binds to ExoQuick-isolated mouse plasma exosomes. To verify the specificity of C1q binding, we fractionated the exosome-bound C1q with OptiPrep Density Gradient (Fig. 5*B*). C1q, TSG101, and mouse IgG were detected in exosomal fraction 9 (1.24 g/mL). The purity of exosomes in fraction 9 was confirmed by the absence of lipoproteins (ApoE and ApoA) and the endoplasmic

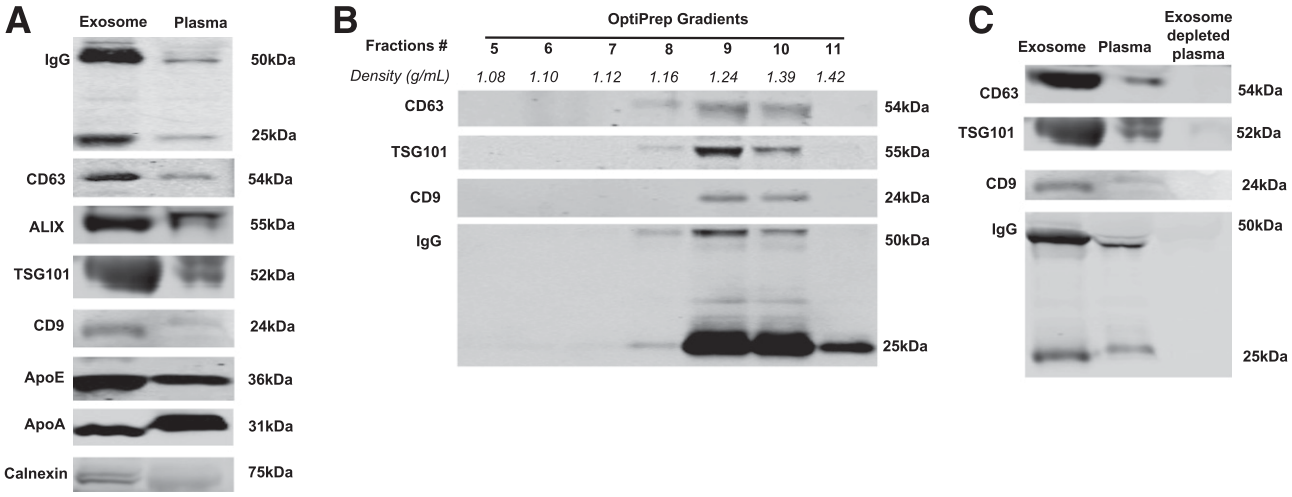

Figure 3—Characterization and specificity of Ig binding to exosomes. *A*: Western blot of exosomes from mouse plasma isolated with ExoQuick, with a 20-μg protein loading volume. Exosomes isolated from mouse plasma showed enrichment of exosomal markers (CD63, ALIX, TSG101, CD9) than whole plasma. Specificity of exosome isolation was confirmed using lipoprotein markers (ApoE and ApoA) and the endoplasmic reticulum marker calnexin. *B*: Western blot of total circulating exosomes. Exosomes were separated with OptiPrep Density Gradient after ExoQuick isolation. The exosomal markers CD63, TSG101, and CD9, as well as Ig, are present in fractions with a density of 1.16–1.39 g/mL (fractions 8–10). *C*: Ig is removed in exosome-depleted plasma (right lane).

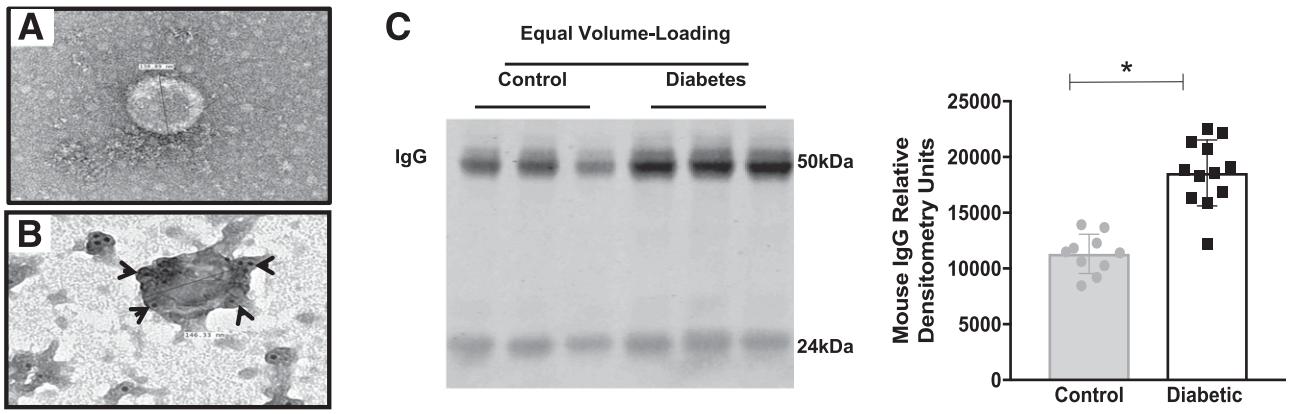

Figure 4—IgG bound to exosomes in plasma and an elevated number of exosomes in diabetes leads to a greater IgG level in mice with diabetes than in control mice. *A* and *B*: TEM images of rat plasma exosomes isolated by ultracentrifugation. A 138.89-nm-diameter exosome was visualized using TEM with uranyl-oxalate staining (*A*). Immunogold-labeled rat IgG colocalized with exosomes (arrowheads) (*B*). *C*: Western blot of mouse plasma exosomes isolated with ExoQuick (left). Under loading conditions of equal volume, more exosomes containing IgG were observed in diabetic mouse plasma (n = 12; white bar, black squares) than in control plasma (n = 10; gray bar, gray circles) (right). Exosomes were quantified on the basis of band intensity. All data points are shown as univariate scatter plots with mean and SD. *$P < 0.05$.

reticulum marker calnexin. We also performed the same experiment using nondiabetic human plasma exosomes and found that endogenous C1q was associated with circulating exosomes and was recognized by antihuman C1q antibody (Fig. 5*C*, left lane). After centrifuging human exosomes with the OptiPrep gradient, we observed that C1q and CD63 were also found in fraction 9 (Fig. 5*D*). C1q was not present alone in any of these fractions (Supplementary Fig. 2).

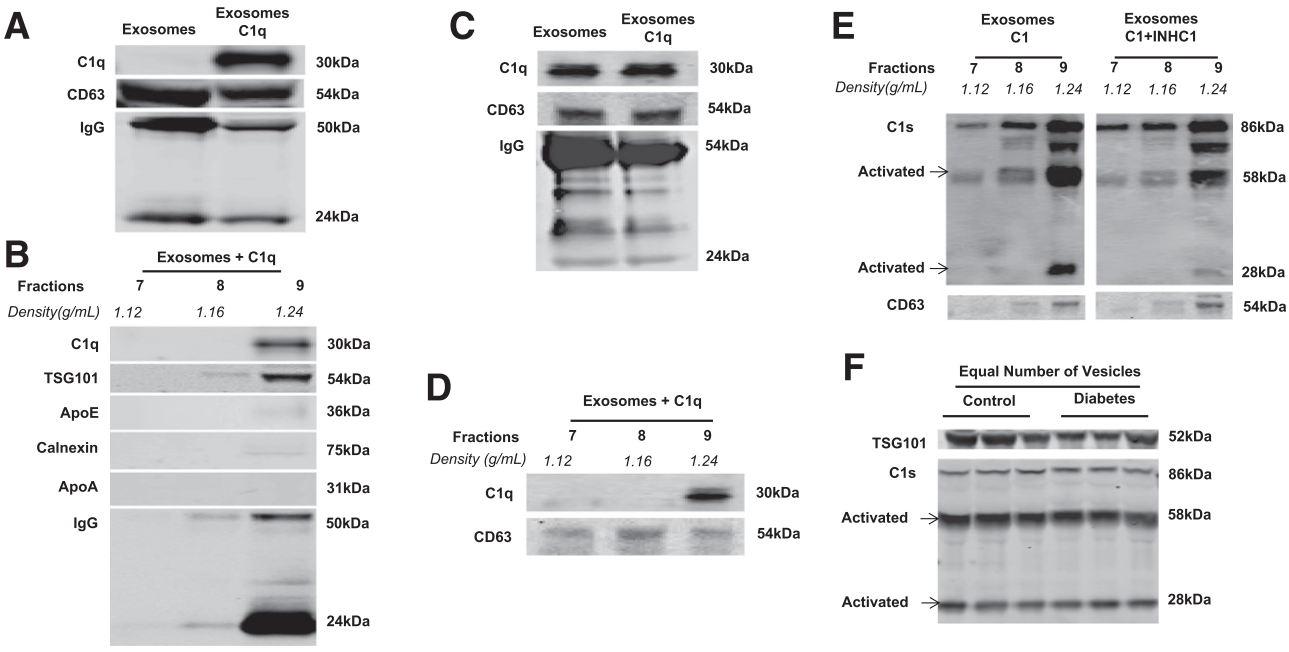

Figure 5—Western blot of complement activation exosomes isolated from mouse and human plasma through ultracentrifugation or ExoQuick and purified with OptiPrep Density Gradient. *A*: Binding of the human complement protein C1q to ExoQuick-isolated mouse exosomes. *B*: C1q specifically bound to mouse plasma exosomes with a density of 1.24 g/mL (fraction 9). This fraction was negative for ApoE, ApoA, and calnexin. *C*: Endogenous human C1q was detected in nondiabetic human plasma exosomes isolated via ultracentrifugation. *D*: After centrifugation in the OptiPrep gradient, human nondiabetic plasma fractions 7–9 were ran. C1q and CD63 were expressed in fraction 9. *E*: C1 was activated by ultracentrifugation-isolated human plasma exosomes. A C1 activation assay was performed by incubating the C1 complex with human plasma exosomes, fractionating them with OptiPrep Density Gradient. The C1 complex bound to exosomes with a 1.24 g/mL density (fraction 9) and activated the serine protease subcomponent C1s (left). The activity of C1s was inhibited by a C1 inhibitor (INHC1) (right). *F*: Under conditions that used an equal number of vesicles, no difference was observed in C1 activation in plasma exomes isolated with ExoQuick from control and STZ-induced diabetic (3 months) mice (n = 3 for both groups).

To investigate whether the binding of C1q to Ig-containing exosomes activates the C1 complex in the classical complement cascade, we performed a C1 activation assay (33). Nondiabetic human exosomes were incubated with C1 complex protein (A098; Complement Technology, Inc.), and C1s was activated in fraction 9 (Fig. 5*E*, left panel). In the presence of a C1 inhibitor (INHC1), however, the activation of C1s was reduced (Fig. 5*E*, right panel). Spontaneous activation of the C1 complex was observed in the reaction (Supplementary Fig. 3); however, spontaneous C1 activation did not occur in fractions without exosomes. Our data demonstrate that binding of C1q to IgG-laden exosomes in plasma causes proteolytic activation of C1 complex. Moreover, under conditions in which an equal number of vesicles are loaded, we found no difference in C1 activation between exosomes from control and those from diabetic mouse plasma (Fig. 5*F*). Thus, these experiments suggest that the elevated number of exosomes observed in diabetes may lead to activation of the classical complement pathway.

Lack of Classical Complement Activation in Diabetic Ighm^{tm1cgn}/J Mice Results in a Reduction of Retinal Vascular Damage

To assess the role of the classical complement pathway in DR, we used a transgenic mouse that lacks complement activator (IgG). Ighm^{tm1cgn}/J (IgM knockout [KO]) is a B-cell-deficient (Ig-deficient) mouse model available from The Jackson Laboratory. These mice lack mature B-cells as a result of a disruption in the heavy chain of IgM, causing B-cell maturation to be arrested at the pre-B-cell stage, which results in lack of IgG production (38). First, we confirmed that IgM-KO mice showed no IgG expression in ExoQuick-isolated plasma exosomes when compared with exosomes from control (C57BL/6J) mice (Fig. 6*A*). Furthermore, we found that exosomes from IgM-KO mice (Fig. 6*B*, right panel) induced less C1 activation than exosomes from C57BL/6J mice (Fig. 6*B*, left panel). To investigate the role of classical complement pathway activation by IgG-laden exosomes in the development of diabetic retinal damage, male IgM-KO and C57BL/6J mice (10–12 weeks old; n = 6) were subjected to STZ-induced diabetes for 7 weeks. Hyperglycemia was observed in both strains of diabetic mice but not in controls. DLS measurement demonstrated that diabetes did not modify exosome size in both strains of mice when compared with nondiabetic controls (Fig. 7*A*). Exosome quantification confirmed that as early as 7 weeks after the onset of diabetes, a higher number of exosomes is found in both strains of mice than in the nondiabetic controls (Fig. 7*B*). A higher number of exosomes in diabetic C57BL/6J mice results in higher IgG levels than in nondiabetic C57BL/6J mice (Fig. 7*C*, left); however, no IgG expression was observed in either control or diabetic IgM-KO plasma exosomes (Fig. 7*C*, right). It is important to note that retinal vascular leakage was reduced in retinas of diabetic IgM-KO mice(Fig. 7*D*, bottom row of images; n = 5) when compared with diabetic retinas from wild-type mice (Fig. 7*D*, top row of images; n = 6). These results suggest that a lack of association of IgG with exosomes prevents exosomes from activating the classical complement pathway, resulting in less diabetes-induced retinal vascular damage.

DISCUSSION

The complement system plays an integral role in both innate and adaptive immune responses. Given the destructive power of complement activation, it is not surprising that aberrant complement system regulation has been shown to be involved in a wide range of diseases, from nonalcoholic steatohepatitis to age-related macular degeneration (39–41). Studies have shown that complement proteins deposited in eyes of patients with diabetes may contribute to the pathogenesis of DR. Mannose-binding lectin and alternative complement pathways have been shown to contribute to complement activation in ocular diseases, including DR (2,36); to our knowledge, however, because of the lack of detection of classical pathway proteins in the retina of patients with DR, no studies have investigated the role of the classical pathway in the pathogenesis of DR. We hypothesize that the classical complement pathway may contribute to DR development via activation on the surface of plasma exosomes, instead of on the lumen of blood vessels. Proteomic studies have shown that classical complement proteins such as C1q, C3, and C4 are associated with isolated plasma exosomes (42–44). In this article we demonstrate that diabetic plasma exosomes activate the classical complement pathway, which leads to downstream retinal vascular damage.

DLS and SLS measurements demonstrated that although the number of exosomes is higher in the plasma of diabetic mice than in that of control mice, the diameter of exosomes is the same in these two groups. Current exosome quantification methods have limitations: for example, conventional flow cytometry cannot discriminate exosomes from background noise; ELISA is limited by the available exosome markers; nanoparticle tracking analysis requires a large sample volume, and the reading is affected by operators (45,46). Among them, DLS/SLS measurement is the most user-friendly and yields relatively accurate and consistent results. It is important to note that these measurements require the smallest sample volume (45–49). A drawback associated with DLS measurement of size is that the technique is more accurate with monodisperse vesicles than with polydisperse vesicles such as plasma exosomes (45–49). Moreover, quantifiable standards are lacking for SLS measurement of exosomes. DLS analysis showed that exosomes isolated from plasma samples are around 100 nm in size. This particle size is consistent with previously reported exosome size measurements and is in close agreement with TEM data. In addition, a standard curve of SLS measurements was generated using extruded lipid vesicles of known diameter and lipid composition to mimic exosomes. Both DLS and TEM measurements confirmed that

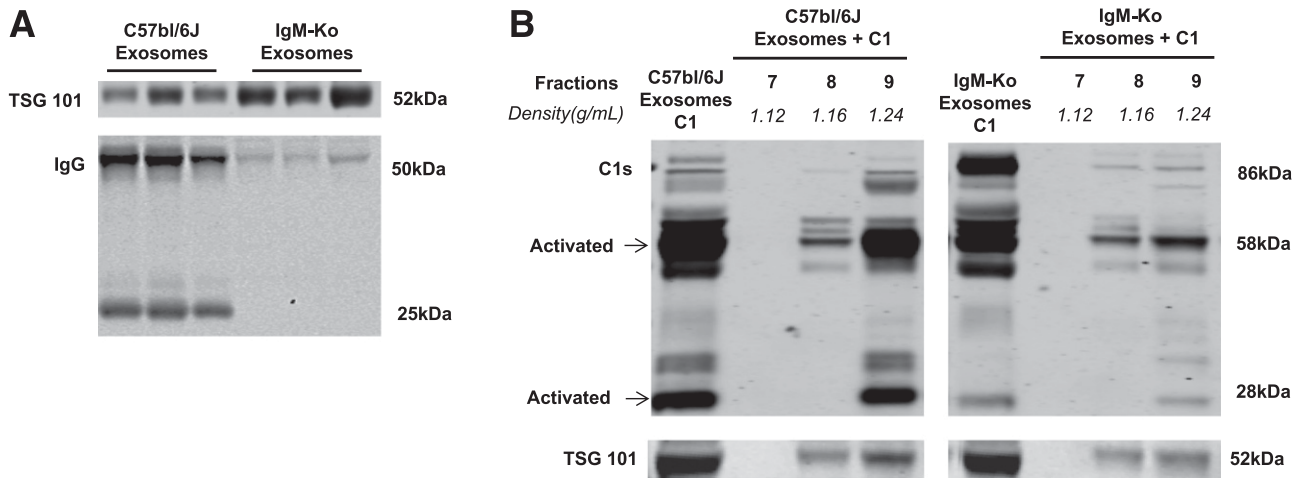

Figure 6—Western blot of plasma exosomes isolated from C57bl/6J and IgM-KO mice with ExoQuick and OptiPrep Density Gradient. *A*: IgM-KO exosomes (right) showed no expression of IgG, but C57bl/6J exosomes did (left). *B*: C1 is activated with exosomes from C57bl/6J mice (left), but not with plasma exosomes from IgM-KO mice (right) (n = 3).

extruded lipid vesicles have a diameter and morphology similar to those of isolated plasma exosomes. Lipid vesicles such as liposomes have been used in previous studies as a model to mimic exosomes and to optimize exosome purification methods and diameter measurement (50,51). Combined DLS/SLS, with extruded vesicles as a standard, may serve as a method to quantify plasma exosomes.

Various exosome isolation methods were used in this study, including polymer-based exosome isolation (ExoQuick), differential ultracentrifugation isolation, and enrichment with OptiPrep Density Gradient. Each isolation method has its own advantages and was used for a different purpose. Ultracentrifugation isolation yields relatively purer exosomes than ExoQuick (36) and works well for exosome characterization, but it requires a larger sample volume. Therefore, in this study ultracentrifugation-isolated rat plasma exosomes were used for immunogold staining to visualize association of plasma exosomes with IgG under TEM. ExoQuick isolation allows for less variation due to sample handling or the isolation process, which is beneficial when comparing exosomes from clinical samples, such as between control and diabetic groups (36). The drawback is that ExoQuick coprecipitates other nonexosomal contaminants such as lipoproteins (LDL, HDL) and cellular organelles (endoplasmic reticulum) (42), which could mask the role of exosomes and confound the study (52,53), thus requiring centrifugation with OptiPrep Density Gradient to further purify the exosome mixture and eliminate most lipoproteins and cellular organelles. Plasma exosomes were isolated by ultracentrifugation followed by centrifugation with OptiPrep Density Gradient in parallel with ExoQuick-OptiPrep to confirm that exosome-induced complement activation is not dependent on the preparation method. This once again demonstrates the drawbacks of each exosome isolation method, calling for more stringent verification of isolated exosomes in future studies and continual development of exosome isolation methods.

Ogata et al. (54) showed that increased levels of extracellular vesicles in diabetic plasma could contribute to accelerated DR progression. Elevated level of serum Ig in diabetes was observed in clinical studies and was suggested to contribute to complications (22,55,56). Consistent with these findings, we observed an increased level of circulating exosomes in diabetes, and we found that exosomes associate with IgG and activate classical complement proteins, suggesting that an elevated number of IgG-laden plasma exosomes in diabetes may result in a greater extent of classical complement activation. To test this hypothesis, we turned to genetically modified mouse models that lack components of this system. C1q-deficient mice develop phenotypes similar to systemic lupus erythematosus or rheumatoid arthritis (57), making it difficult to differentiate damage induced by C1q deficiency versus that induced by diabetes. The B-cell-deficient (IgM-KO) mouse model, on the other hand, does not have this complication. Moreover, the IgM-KO mouse model specifically lacks circulating IgG—the rest of the complement proteins are intact—helping us to address the hypothesis that it is the IgG-laden exosomes that contribute to diabetes-induced complement activation. On the basis of these considerations, we used the IgM-KO mouse model in this study. After STZ induction of diabetes, IgM-KO mice developed hyperglycemia at the same rate and with the same severity as wild-type C57BL/6J mice. Moreover, diabetic IgM-KO mice had more exosomes than their littermate controls, similar to diabetic C57BL/6J mice. Despite the increase in the number of exosomes in diabetic IgM-KO mice, the exosomes from IgM-KO mice lacked IgG and had very low levels of C1 activation when compared with C57BL/6J exosomes.

In biological fluids such as plasma, exosome populations are highly heterogeneous and originate from various cell

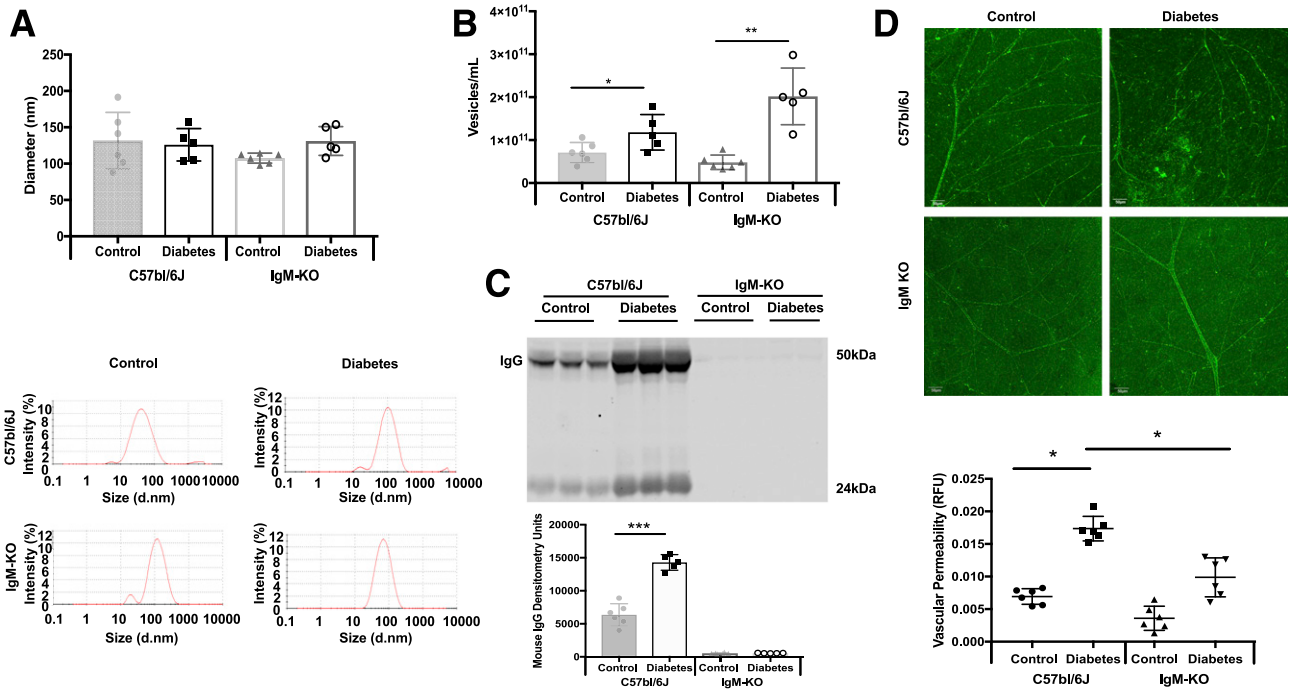

Figure 7—Analysis of plasma exosomes, isolated with ExoQuick, from control and STZ-induced diabetic (7 weeks) C57BL/6J and IgM-KO mice. *A*: DLS measurements showed no difference in the diameter of plasma exosomes from C57bl/6J and IgM-KO control (gray bar, gray circles, and white bar, black squares, respectively) or C57bl/6J or IgM-KO diabetic mice (white bar, gray triangles and white bar, white circles, respectively). *B*: The number of plasma exosomes was increased significantly in both C57bl/6J and IgM-KO diabetic mice compared to control (symbols as in *A*) . Exosomes were isolated with ExoQuick from plasma from control ($n = 6$) and STZ-induced diabetic ($n = 5$) mice and measured by using SLS (kilocounts per second). $^*P < 0.05$; $^{**}P < 0.01$. *C*: Western blot of ExoQuick-isolated mouse plasma exosomes (top). Under loading conditions of equal volume, more diabetic C57bl/6J plasma exosomes contained IgG (white bar) than control plasma exosomes (gray bar) (bottom). No IgG expression was measured within IgM-KO control or diabetic plasma exosomes. $^{***}P < 0.001$. *D*: Retinal permeability was examined in control and diabetic C57bl/6J and IgM-KO mice (7 weeks control and diabetes; $n = 6$). Diabetic C57bl/6J retinas showed more vascular permeability than control retinas (top), but retinal vascular permeability in IgM-KO mice did not significantly change between the control and diabetes states (bottom). Retinal fluorescence intensity is quantified through the use of fluorescein isothiocyanate–albumin, as shown in the graph at the bottom (control, $n = 6$; diabetes, $n = 5$; black circles = C57bl/6J control, black squares = C57bl/6J diabetic; black triangles = IgM-KO control; black inverted triangles = IgM-KO diabetic). Scale bars = 50 μm. All data points are presented as univariate scatter plots with mean and SD. d.nm., diameter, in nanometers; RFU, relative fluorescent unit.

types. Saunderson et al. (58) reported that Igs are enriched in exosomes released by primary B-cells and suggested that Igs present on the B-cell plasma membrane could be shuttled into exosomes. On the other hand, Blanc et al. (21) demonstrated that reticulocyte-secreted exosomes have a natural affinity for Igs in blood. These findings suggest distinct possibilities for IgG association with exosomes: as primary secretion of IgG packaged inside the exosomes of IgG-producing B-cells, or as a secondary association of exosomes, potentially produced by multiple cell types, with circulating Igs in blood. Because complement complex C1 binding and activation require surface presentation of IgG, only the exosomes with surface IgG would contribute to activation. Indeed, we observed that only a fraction of the IgG-associated exosomes of specific density activate complement complex C1. Diebolder et al. (59) reported that the presentation of the Fc-Fc segment of IgG hexamers drives classical complement C1 activation. On the basis of that finding, we speculate that a subpopulation of exosomes that activate the C1 complex may present the Fc motif, which favors activation of the classical complement pathway. It is notable that the exosome subpopulation that activated C1 in our study was found to be enriched with several exosomal markers: CD63, TSG101, and CD9. These markers were shown to be directly involved in different exosomal cargo-sorting processes in the endosomal compartment (60,61). TSG101 is a component of the endosomal sorting complexes required for transport (ESCRT) complex, which participates in ESCRT-dependent exosome biogenesis (61). By contrast, the tetraspanin family proteins CD63 and CD9 are responsible for ESCRT-independent exosome biogenesis (60). These two exosomal biogenesis mechanisms can act independently or simultaneously within an endosomal compartment, generating highly complex and heterogeneous exosomal populations (60). Exosomes found within fraction 9 are likely to be a mixed population generated by a combination of exosomal biogenesis mechanisms. These data are in agreement with those from a recent study showing that retinal pigment epithelium–derived vesicles in fraction 9 contain complement components (13).

Under normal conditions, a low level of complement activation protects the eye from pathogenic infection. This process is tightly controlled by complement regulatory

proteins, which prevent complement-induced self-destruction (62). In diabetes, protein glycosylation and hyperglycemic by-products greatly reduce the function of complement regulatory proteins in the circulation and on cell membranes (10,63), suggesting that spontaneous alternative complement activation plays a role in MAC (C5b-9)–induced retinal vascular damage (2,7). In addition, formation of cytolytic MAC leads to osmotic imbalance and, ultimately, to cell lysis. Extensive deposition of MAC in the retinal endothelium of patients with DR and in rats with diabetes could contribute to retinal endothelial cell death and the resulting retinal vasculature leakage (8). We used IgM-KO mice to demonstrate that an increase in classical complement activation by IgG-laden exosomes under diabetic conditions may contribute to retinal vascular damage and increased permeability of the retina. As discussed above, although IgM-KO mice develop STZ-induced diabetes and have more exosomes in circulation, those exosomes lack IgG and do not activate the classical complement pathway. As expected, C57BL/6J mice had significantly increased retinal vascular leakage after 7 weeks of diabetes; however, this increase in retinal vascular leakage was abolished in diabetic IgM-KO mice despite the same degree of hyperglycemia.

In conclusion, this study demonstrates that diabetic plasma exosomes are a part of the circulating microenvironment responsible for activation of the complement cascade, which in turn leads to the upregulation of proinflammatory cytokines and chemokines, resulting in vascular damage. Inhibition of exosome-induced complement pathway activation could prevent the advancement of DR pathogenesis.

Acknowledgments. The authors acknowledge the Investigative HistoPathology Laboratory, Center for Advanced Microscopy, Michigan State University.

Funding. This research was supported by Michigan Experimental Agricultural Station (grant no. MICL02163) and the National Institutes of Health (grant nos. R01EY016077 and R01EY025383 to J.V.B.).

Duality of Interest. No potential conflicts of interest relevant to this article were reported.

Author Contributions. C.H. designed and performed the experiment, analyzed and interpreted the data, and wrote the manuscript. K.P.F. and S.S.H. performed experiments, reviewed the manuscript, and contributed to the discussion. S.N. performed experiments. G.J.B. quantified exosomes and reviewed the manuscript. J.V.B. designed the experiment, performed the study, and reviewed and edited the manuscript. J.V.B. is the guarantor of this work and, as such, had full access to all the data in the study and takes responsibility for the integrity of the data and the accuracy of the data analysis.

References

1. Jha P, Bora PS, Sohn JH, Kaplan HJ, Bora NS. Complement system and the eye. Adv Exp Med Biol 2006;586:53–62

2. Yanai R, Thanos A, Connor KM. Complement involvement in neovascular ocular diseases. In *Current Topics in Innate Immunity II*. Lambris JD, Ed. New York, Springer, 2012, p. 161–183

3. Joussen AM, Murata T, Tsujikawa A, Kirchhof B, Bursell SE, Adamis AP. Leukocyte-mediated endothelial cell injury and death in the diabetic retina. Am J Pathol 2001;158:147–152

4. Bora NS, Jha P, Bora PS. The role of complement in ocular pathology. Semin Immunopathol 2008;30:85–95

5. Clark SJ, Bishop PN. The eye as a complement dysregulation hotspot. Semin Immunopathol 2018;40:65–74

6. Walport MJ. Complement. First of two parts. N Engl J Med 2001;344:1058–1066

7. Gerl V, Bohl J, Pitz S, Stoffelns B. Extensive deposits of complement C3d and C5b-9 in the choriocapillaris of eyes of patients with diabetic retinopathy. Invest Ophthalmol Vis Sci 2002;43:1104–1108

8. Zhang J, Gerhardinger C, Lorenzi M. Early complement activation and decreased levels of glycosylphosphatidylinositol-anchored complement inhibitors in human and experimental diabetic retinopathy. Diabetes 2002;51:3499–3504

9. García-Ramírez M, Canals F, Hernández C, et al. Proteomic analysis of human vitreous fluid by fluorescence-based difference gel electrophoresis (DIGE): a new strategy for identifying potential candidates in the pathogenesis of proliferative diabetic retinopathy. Diabetologia 2007;50:1294–1303

10. Aleksandrovskii YA. Antithrombin III, C1 inhibitor, methylglyoxal, and polymorphonuclear leukocytes in the development of vascular complications in diabetes mellitus. Thromb Res 1992;67:179–189

11. Looze C, Yui D, Leung L, et al. Proteomic profiling of human plasma exosomes identifies PPARgamma as an exosome-associated protein. Biochem Biophys Res Commun 2009;378:433–438

12. Kowal J, Arras G, Colombo M, et al. Proteomic comparison defines novel markers to characterize heterogeneous populations of extracellular vesicle subtypes. Proc Natl Acad Sci U S A 2016;113:E968–E977

13. Klingeborn M, Dismuke WM, Skiba NP, Kelly U, Stamer WD, Bowes Rickman C. Directional exosome proteomes reflect polarity-specific functions in retinal pigmented epithelium monolayers. Sci Rep 2017;7:4901

14. Caby M-P, Lankar D, Vincendeau-Scherrer C, Raposo G, Bonnerot C. Exosomal-like vesicles are present in human blood plasma. Int Immunol 2005;17:879–887

15. Muller L, Hong C-S, Stolz DB, Watkins SC, Whiteside TL. Isolation of biologically-active exosomes from human plasma. J Immunol Methods 2014;411:55–65

16. Zubiri I, Posada-Ayala M, Sanz-Maroto A, et al. Diabetic nephropathy induces changes in the proteome of human urinary exosomes as revealed by label-free comparative analysis. J Proteomics 2014;96:92–102

17. Urbanelli L, Magini A, Buratta S, et al. Signaling pathways in exosomes biogenesis, secretion and fate. Genes (Basel) 2013;4:152–170

18. Simpson RJ, Lim JW, Moritz RL, Mathivanan S. Exosomes: proteomic insights and diagnostic potential. Expert Rev Proteomics 2009;6:267–283

19. Pan BT, Johnstone RM. Fate of the transferrin receptor during maturation of sheep reticulocytes in vitro: selective externalization of the receptor. Cell 1983;33:967–978

20. Hajrasouliha AR, Jiang G, Lu Q, et al. Exosomes from retinal astrocytes contain antiangiogenic components that inhibit laser-induced choroidal neovascularization. J Biol Chem 2013;288:28058–28067

21. Blanc L, Barres C, Bette-Bobillo P, Vidal M. Reticulocyte-secreted exosomes bind natural IgM antibodies: involvement of a ROS-activatable endosomal phospholipase iPLA2. Blood 2007;110:3407–3416

22. Rodriguez-Segade S, Camiña MF, Carnero A, et al. High serum IgA concentrations in patients with diabetes mellitus: agewise distribution and relation to chronic complications. Clin Chem 1996;42:1064–1067

23. Rossini AA, Like AA, Chick WL, Appel MC, Cahill GF Jr. Studies of streptozotocin-induced insulitis and diabetes. Proc Natl Acad Sci U S A 1977;74:2485–2489

24. Kady N, Liu X, Lydic TA, et al. ELOVL4-mediated production of very long-chain ceramides stabilizes tight junctions and prevents diabetes-induced retinal vascular permeability. Diabetes 2018;67:769–781

25. Opreanu M, Lydic TA, Reid GE, McSorley KM, Esselman WJ, Busik JV. Inhibition of cytokine signaling in human retinal endothelial cells through downregulation of sphingomyelinases by docosahexaenoic acid. Invest Ophthalmol Vis Sci 2010;51:3253–3263

26. Théry C, Amigorena S, Raposo G, Clayton A. Isolation and characterization of exosomes from cell culture supernatants and biological fluids. Curr Protoc Cell Biol 2006;Chapter 3:Unit 3.22
27. Tauro BJ, Greening DW, Mathias RA, et al. Comparison of ultracentrifugation, density gradient separation, and immunoaffinity capture methods for isolating human colon cancer cell line LIM1863-derived exosomes. Methods 2012;56:293–304
28. Schröder M, Schäfer R, Friedl P. Spectrophotometric determination of iodixanol in subcellular fractions of mammalian cells. Anal Biochem 1997;244:174–176
29. Lydic TA, Townsend S, Adda CG, Collins C, Mathivanan S, Reid GE. Rapid and comprehensive "shotgun" lipidome profiling of colorectal cancer cell derived exosome. Methods 2015;87:83–95
30. Bradley AJ, Brooks DE, Norris-Jones R, Devine DV. C1q binding to liposomes is surface charge dependent and is inhibited by peptides consisting of residues 14-26 of the human C1qA chain in a sequence independent manner. Biochim Biophys Acta 1999;1418:19–30
31. Nydegger UE, Lambert PH, Gerber H, Miescher PA. Circulating immune complexes in the serum in systemic lupus erythematosus and in carriers of hepatitis B antigen. Quantitation by binding to radiolabeled C1q. J Clin Invest 1974; 54:297–309
32. Biró A, Thielens NM, Cervenák L, Prohászka Z, Füst G, Arlaud GJ. Modified low density lipoproteins differentially bind and activate the C1 complex of complement. Mol Immunol 2007;44:1169–1177
33. Biro A, Ling WL, Arlaud GJ. Complement protein C1q recognizes enzymatically modified low-density lipoprotein through unesterified fatty acids generated by cholesterol esterase. Biochemistry 2010;49:2167–2176
34. Lobb RJ, Becker M, Wen SW, et al. Optimized exosome isolation protocol for cell culture supernatant and human plasma. J Extracell Vesicles 2015;4:27031
35. Witwer KW, Buzás EI, Bemis LT, et al. Standardization of sample collection, isolation and analysis methods in extracellular vesicle research. J Extracell Vesicles 2013;2:1–25
36. Li P, Kaslan M, Lee SH, Yao J, Gao Z. Progress in exosome isolation techniques. Theranostics 2017;7:789–804
37. Zubler RH, Lange G, Lambert PH, Miescher PA. Detection of immune complexes in unheated sera by modified 125I-Clq binding test. Effect of heating on the binding of Clq by immune complexes and application of the test to systemic lupus erythematosus. J Immunol 1976;116:232–235
38. Kitamura D, Roes J, Kühn R, Rajewsky K. A B cell-deficient mouse by targeted disruption of the membrane exon of the immunoglobulin mu chain gene. Nature 1991;350:423–426
39. Girmens JF, Sahel JA, Marazova K. Dry age-related macular degeneration: a currently unmet clinical need. Intractable Rare Dis Res 2012;1:103–114
40. Rensen SS, Slaats Y, Driessen A, et al. Activation of the complement system in human nonalcoholic fatty liver disease. Hepatology 2009;50:1809–1817
41. Couser WG, Johnson RJ. The etiology of glomerulonephritis: roles of infection and autoimmunity. Kidney Int 2014;86:905–914
42. Kalra H, Adda CG, Liem M, et al. Comparative proteomics evaluation of plasma exosome isolation techniques and assessment of the stability of exosomes in normal human blood plasma. Proteomics 2013;13:3354–3364
43. Xu H, Chen M. Targeting the complement system for the management of retinal inflammatory and degenerative diseases. Eur J Pharmacol 2016;787:94–104
44. Simpson RJ, Kalra H, Mathivanan S. ExoCarta as a resource for exosomal research. J Extracell Vesicles 2012;1:1–6
45. Maas SLN, de Vrij J, van der Vlist EJ, et al. Possibilities and limitations of current technologies for quantification of biological extracellular vesicles and synthetic mimics. J Control Release 2015;200:87–96
46. Palmieri V, Lucchetti D, Gatto I, et al. Dynamic light scattering for the characterization and counting of extracellular vesicles: a powerful noninvasive tool. J Nanopart Res 2014;16:2583
47. van der Pol E, Hoekstra AG, Sturk A, Otto C, van Leeuwen TG, Nieuwland R. Optical and non-optical methods for detection and characterization of microparticles and exosomes. J Thromb Haemost 2010;8:2596–2607
48. Filipe V, Hawe A, Jiskoot W. Critical evaluation of Nanoparticle Tracking Analysis (NTA) by NanoSight for the measurement of nanoparticles and protein aggregates. Pharm Res 2010;27:796–810
49. Bootz A, Vogel V, Schubert D, Kreuter J. Comparison of scanning electron microscopy, dynamic light scattering and analytical ultracentrifugation for the sizing of poly(butyl cyanoacrylate) nanoparticles. Eur J Pharm Biopharm 2004;57: 369–375
50. Jin AJ, Huster D, Gawrisch K, Nossal R. Light scattering characterization of extruded lipid vesicles. Eur Biophys J 1999;28:187–199
51. Lane RE, Korbie D, Anderson W, Vaidyanathan R, Trau M. Analysis of exosome purification methods using a model liposome system and tunable-resistive pulse sensing. Sci Rep 2015;5:7639
52. Zarovni N, Corrado A, Guazzi P, et al. Integrated isolation and quantitative analysis of exosome shuttled proteins and nucleic acids using immunocapture approaches. Methods 2015;87:46–58
53. Jorge I, Burillo E, Mesa R, et al. The human HDL proteome displays high inter-individual variability and is altered dynamically in response to angioplasty-induced atheroma plaque rupture. J Proteomics 2014;106:61–73
54. Ogata N, Imaizumi M, Nomura S, et al. Increased levels of platelet-derived microparticles in patients with diabetic retinopathy. Diabetes Res Clin Pract 2005; 68:193–201
55. Zhang L, Li Y, Payne J, et al. Presence of retinal pericyte-reactive autoantibodies in diabetic retinopathy patients. Sci Rep 2016;6:20341
56. Ardawi MS, Nasrat HA, Bahnassy AA. Serum immunoglobulin concentrations in diabetic patients. Diabet Med 1994;11:384–387
57. Mitchell DA, Pickering MC, Warren J, et al. C1q deficiency and autoimmunity: the effects of genetic background on disease expression. J Immunol 2002;168:2538–2543
58. Saunderson SC, Schuberth PC, Dunn AC, et al. Induction of exosome release in primary B cells stimulated via CD40 and the IL-4 receptor. J Immunol 2008;180:8146–8152
59. Diebolder CA. Beurskens FJ, de Jong RN, et al. Complement is activated by IgG hexamers assembled at the cell surface. Science 2014;343:1260–1263
60. Colombo M, Raposo G, Théry C. Biogenesis, secretion, and intercellular interactions of exosomes and other extracellular vesicles. Annu Rev Cell Dev Biol 2014;30:255–289
61. van Niel G, D'Angelo GR, Raposo G. Shedding light on the cell biology of extracellular vesicles. Nat Rev Mol Cell Biol 2018;19:213–228
62. Sohn JH, Kaplan HJ, Suk HJ, Bora PS, Bora NS. Chronic low level complement activation within the eye is controlled by intraocular complement regulatory proteins. Invest Ophthalmol Vis Sci 2000;41:3492–3502
63. Qin X, Goldfine A, Krumrei N, et al. Glycation inactivation of the complement regulatory protein CD59: a possible role in the pathogenesis of the vascular complications of human diabetes. Diabetes 2004;53:2653–2661